This copy of the ESI was uploaded on 13th October 2022, replacing any previous versions published on 20th March 2012

Electronic Supplementary Information: *Photolysis of T-butylnitrite via Excitation to the S_1 and S_2 States Studied by Velocity-Map Ion-Imaging & 3D-REMPI Spectroscopy*

1. Apparatus & Ion-Optics Design

1.1 Vacuum Apparatus

The new built VMI apparatus using the SolidEdge CAD software package[1], is optimized regarding vacuum, maintenance and adjustability (cf. Figure 1). To ensure a possible maximum of image resolution, the assembly of nozzle, skimmer and ion optics can be mechanically aligned to the center of the detector using the precision adjustment screws without changing the ideal region for photolysis and ionization. This is achieved by placing the turning point of the whole unit (mounted in a PEEK/graphite bowl) at the ideal crossing between the molecular beam and the lasers, which is halfway between the repeller and extractor electrode. The high voltage supply (0-8 kV) is connected by a self-attaching/detaching unit to a connector plate on the electrodes assembly. The nozzle, skimmer and ion optics assembly can be removed and remounted from the setup through the source chamber flange without accessing the interaction or TOF/detector chamber.

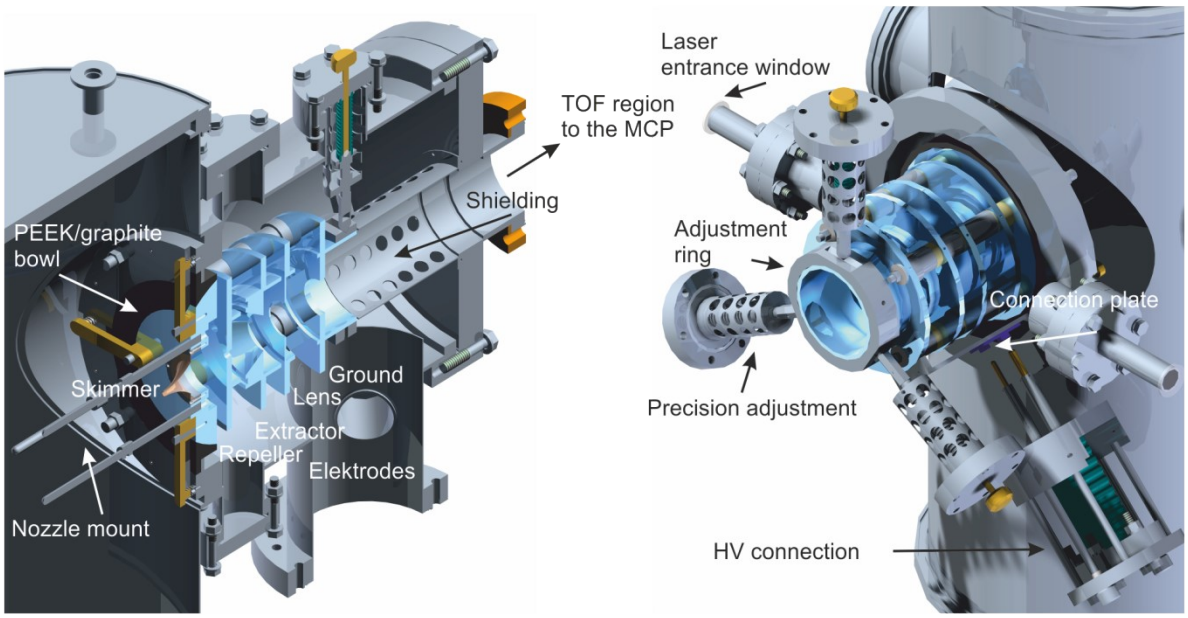

Figure 1 Schematics of the main features of the new build VMI apparatus.

1.2 Ion optics

The ion optics (Figure 2) were fully revised and are based on a previous work of Wrede *et al.*.[2] The optimal voltage ratios of the different electrodes were obtained by minimizing the focal diameter of three NO^+ ions starting in the interaction volume with 1 mm spacing and a velocity vector perpendicular to the TOF axis. As an additional constrain the ions´ trajectories must not cross during the flight. Only one global minimum on the focal diameter hypersurface exists, which fulfills this constrain. Therefore the ion optics are fully characterized by the voltage ratios: $U_R : U_E : U_L = 1 : 0.803 : 0.246$.

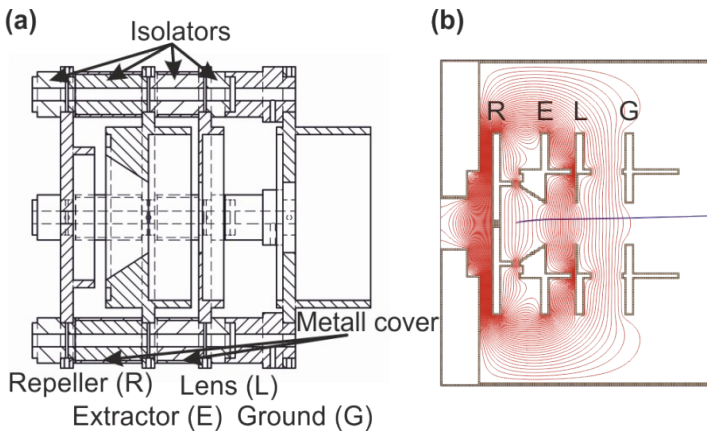

Figure 2(a) Schematics of the new constructed optimized ion-optics. (b) Potential curves obtained with the SIMION software package. The optimized voltage ratios are $U_R : U_E : U_L = 1 : 0.803 : 0.246$. The blue lines indicate the trajectories.

2. Velocity calibration

To obtain the function for the velocity calibration of the VMI setup the photodissociation reaction $NO_2 + h\nu \rightarrow NO_2((2)^2B_2) \rightarrow O(^1D_2) + NO(^2\Pi_\Omega, v, j; \Omega=1/2, 3/2)$ was used. The velocity v_i of a certain photolysis fragment *i* (here: NO) is proportional to the radius r_i following the equations:

$$v_i = k \cdot \sqrt{\frac{z \cdot U_R}{M}} \cdot r_i \tag{1}$$

$$v_{rms}^{NO} = \sqrt{\frac{2\left(E_{ph} - D_0 - E_{int}^{NO} - E_{el}^{O}\right)}{m_{NO}\left(1 + \frac{m_{NO}}{m_O}\right)}} \tag{2}$$

The radius r_i can be obtained by the reconstruction of the three dimensional fragment distri-

bution out of the ion images using a various type of methods.[3-13] The images, chosen for the velocity calibration all possessed O($^1D_2$) as counter fragment. Furthermore the NO internal energy (E_{int}^{NO}) can be calculated following the equations

$$E_{int}^{NO} = E_{vib}^{NO} + E_{rot}^{NO} \tag{3}$$

$$E_{vib}^{NO}(v) = \bar{v}\left(\mu'' + \frac{1}{2}\right) - \bar{v}x_e\left(v + \frac{1}{2}\right)^2 - \bar{v}y_e\left(v + \frac{1}{2}\right)^3 - E_{vib}^{NO}(0) \tag{4}$$

$$E_{rot}^{NO}(v,j) = B_v\left[\left(j - \frac{1}{2}\right)\left(j + \frac{3}{2}\right) \pm \frac{1}{2}X\right] \tag{5}$$

$$B_v = B_e - \alpha_e\left(v + \frac{1}{2}\right) \tag{6}$$

$$X = \left[4\left(j + \frac{1}{2}\right)^2 + \frac{A_v}{B_e - \alpha_e\left(v + \frac{1}{2}\right)}\left(\frac{A_v}{B_e - \alpha_e\left(v + \frac{1}{2}\right)} - 4\right)\right]^{\frac{1}{2}} \tag{7}$$

where the occurrence of the two different spin-orbit states NO($^2\Pi\Omega$, v, j; Ω=1/2, 3/2) and the therefore different electronic energies E_{el}^{NO} are taken into account by setting a virtual level $E_{el,virt}^{NO} = 0\ \mathrm{cm}^1$ correcting the rotational energy according the corresponding spin-orbit state. For the NO($^2\Pi_{1/2}$) spin-orbit state the minus in eqn. 5 is applied whereas the plus is used for NO($^2\Pi_{3/2}$), respectively.[14, 15] All relevant constants are listed in Table 1. Due to the fact, that the imaging properties of ion optics of the Wrede *et al.* type lose their linearity for small radii *r* (not depending on the applied acceleration voltage) the calibration constant *k* should be modified to get a good description for all radii (Figure 3).

$$k = k_0 + k_1 \cdot e^{-\left(\frac{r}{r_0}\right)} \tag{8}$$

The calibration constant of the described setup can be calculated:

For *r* > 125 pixel *k* can be treated as a constant because of the linearity between *v* and *r* (see Figure 3).

$$k = 0.913 \pm 0.001\sqrt{\frac{As}{kmol}}pixel^{-1} \tag{9}$$

For a good description of the whole range of *r*:

$$k_0 = 0.912 \pm 0.001 \sqrt{\frac{As}{kmol}} pixel^{-1} \tag{10}$$

$$k_1 = 1.1 \pm 0.3 \sqrt{\frac{As}{kmol}} pixel^{-1} \tag{11}$$

$$r_0 = 29 \pm 3\, pixel \tag{12}$$

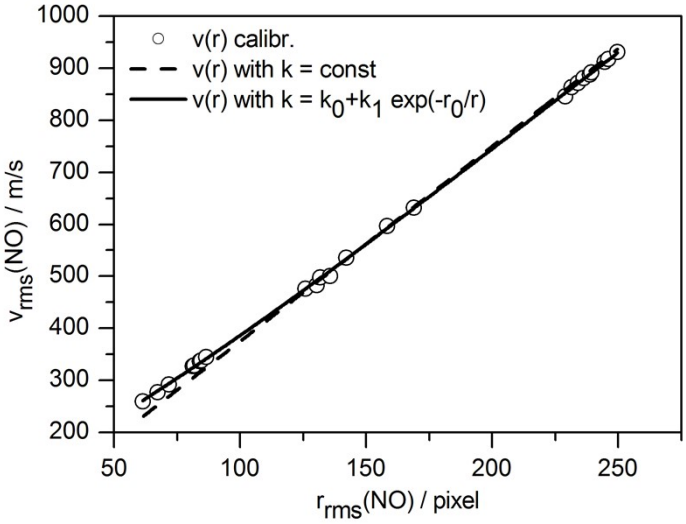

Figure 3 Velocity *vs.* radius calibration of the VMI apparatus. The photodissociation of NO_2 via its $(2)^2B_2$ with $O(^1D_2)$ as counter fragment is used as model system. The applied total voltage U_R is 500 V. The open circles show the experimental obtained dependence radius *vs.* velocity. The linear calibration (*i.e. k* is constant for all radii) is represented by the dashed and the exponential (eqn. 8) by the solid line.

Table 1 Necessary constants for the velocity calibration: m_i mass of the corresponding fragment, E_{el}^{O} ($^1D_2$) electronic energy of oxygen in its first excited state, D_0 dissociation energy of NO_2. $\bar{\nu}$, x_e, y_e, B_e, α_e and A_v are molecular constants for the calculation of the rovibrational energies of NO. [14, 15]

Parameter	Values
m_{NO} / kg	$4.983 \cdot 10^{-26}$
M_{NO} / kg	30.006
m_O / g/mol	$2.657 \cdot 10^{-26}$
E_{el}^{O} ($^1D_2$) / cm^{-1}	15867.9
D_0 / cm^{-1}	25130.6
$\bar{\nu}$ / cm^{-1}	1903.5
x_e	$7.3391 \cdot 10^{-3}$
y_e	$6.33042 \cdot 10^{-7}$
B_e	1.7046
α_e	0.0178
A_v / cm^{-1}	123.03716

3. Mass calibration

The calibration of the fragment mass to its flight time t_{TOF} allows mass selective experiments by applying the MCP high voltage only in a specific time window. The following equation gives a relation between t_{TOF}, the ion mass m and charge q and the applied voltage U_R of the ion optics.

$$t_{TOF} = a_1 \cdot \sqrt{\frac{m}{qU_R}} + a_2 \tag{13}$$

The linearity of this relation can be reviewed in Figure 4 and is in excellent agreement with the TOF simulation obtained from SIMION. The discrepancy in the TOF axis intercept can be explained by the different time zero point (t_{TOF} = 0 µs) between experiment und simulation. The calibration parameter can therefore be fitted to

$$a_1 = 4.223 \cdot 10^5 \pm 9\, m \tag{14}$$

$$a_2 = -3 \cdot 10^{-3} \pm 0.06 \cdot 10^{-3}\, \mu s \tag{15}$$

And used for mass selective measurements.

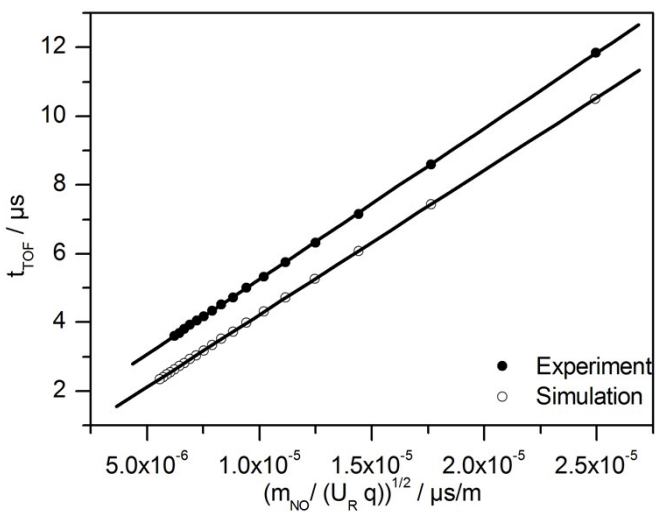

Figure 4 Time of flight calibration. The simulation (open circles) is in excellent agreement with the experimental results (full circles). The parameters from the linear fit can be used for mass selective measurements.

4. Calculations

4.1 *t*-BuONO dissociation energy

The dissociation energy of a system AB is calculated from the following contributions:

This copy of the ESI was uploaded on 13th October 2022, replacing any previous versions published on 20th March 2012

Table 2 Required values for calculation the dissociation energy of a system AB.

Parameter	Description
AB_{opt}	Optimized energy of the complete system.
A(B)	Energy of system A in presence of orbitals of system B at AB_{opt} geometry.
(A)B	Energy of system B in presence of orbitals of system A at AB_{opt} geometry.
A_{fix}	Energy of system A at fixed AB_{opt} geometry.
B_{fix}	Energy of system B at fixed AB_{opt} geometry.
A_{opt}	Energy of system A at optimized geometry.
B_{opt}	Energy of system B at optimized geometry.

Then DE_{opt} is the uncorrected dissociation energy as difference between the optimized energies, *BSSE* is the basis set superposition contribution, and $DE_{CP\text{-}corr}$ is the dissociation energy with counterpoise correction.

$$DE_{opt} = A_{opt} + B_{opt} - AB_{opt} \tag{16}$$

$$BSSE = A_{fix} + B_{fix} - A(B) - (A)B \tag{17}$$

$$DE_{CP-corr} = DE_{opt} - BSSE \tag{18}$$

Table 3 Calculated dissociation energy for *t*-BuONO. Upper part: energies in Hartree units, lower part: cm^{-1} units.

	CCD	ACCD	ACCT	extrap.
Hartree:				
t-BuONO *opt*	-362.983200	-363.015865	-363.110590	
t-BuO(NO)	-233.013753	-233.033448	-233.098373	
(*t*-BuO)NO	-129.903488	-129.913183	-129.942316	
t-BuO *fix*	-233.011048	-233.032478	-233.098252	
NO *fix*	-129.900670	-129.912615	-129.941962	
t-BuO *opt*	-233.014504	-233.036409	-233.102234	
NO *opt*	-129.901862	-129.914219	-129.943585	
DE_{opt}	0.066834	0.065237	0.064770	
BSSE	0.005523	0.001538	0.000475	
$DE_{CP\text{-}corr}$	0.061310	0.063699	0.064295	
cm^{-1}:				
BSSE	**1212.2**	**337.5**	**104.3**	**0.0**
$DE_{CP\text{-}corr}$	13456.1	13980.2	14111.1	14176.3
ZPE				
t-BuONO	28741.5	28783.9	28837.3	
t-BuO	26582.4	26624.4	26582.4	
NO	996.6	996.5	987.4	

This copy of the ESI was uploaded on 13th October 2022, replacing any previous versions published on 20th March 2012

D_{ZPE}	1162.6	1163.0	1267.5	
DE_0	**12293.5**	**12817.3**	**12843.7**	**12908.8**

Extrapolation to infinite basis (*i.e.* to zero *BSSE*)

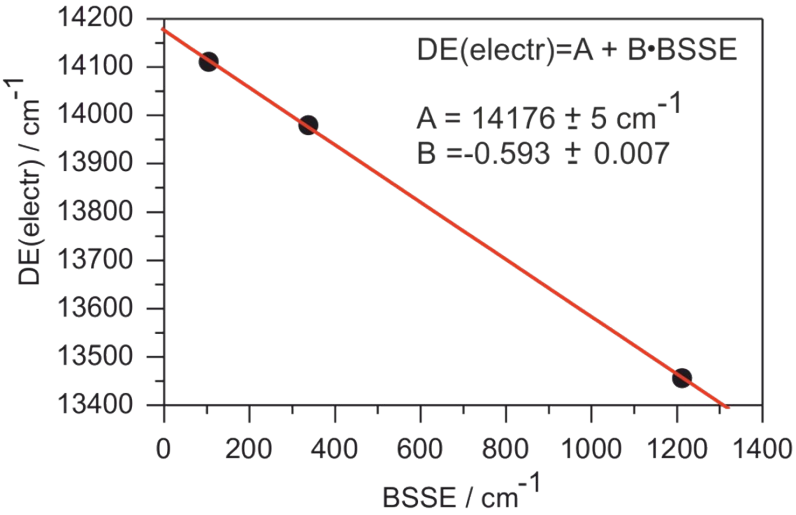

Figure 5 Extrapolation of the *t*-BuONO dissociation energy *vs. BSSE* to an infinite basis.

4.2 Ground state and excitation energies

T-BuONO can exist in two different conformers label as *syn* and *anti*. The results of the energy difference between the isomers are depicted in Table 4.

Table 4 Calculated energy differences between the rotational isomers of *t*-BuONO.

	CCD	ACCD	ACCT

This copy of the ESI was uploaded on 13th October 2022, replacing any previous versions published on 20th March 2012

Hartree:			
syn	-362.980582	-363.010661	-363.105163
anti	-362.983200	-363.015864	-363.110590
ZPE/cm^{-1}:			
syn	28797.4	28817.1	28868.5
anti	28741.5	28783.8	28837.3
DE(syn-anti)	**630.5**	**1175.2**	**1222.3**

This copy of the ESI was uploaded on 13th October 2022, replacing any previous versions published on 20th March 2012

Excitation energies: *Anti* conformer:

Table 5: Calculated excitation energies for the anti-conformer of *t*-BuONO.

CCD:

TDDFT EXCITATION ENERGIES

STATE	HARTREE	EV	KCAL/MOL	CM^{-1}	NANOMETERS	OSC. STR.
1A''	0.1193652280	3.2481	74.9028	26197.64	381.71	0.0015010
1A'	0.2086649059	5.6781	130.9392	45796.65	218.36	0.0533755
1A''	0.2260916548	6.1523	141.8747	49621.38	201.53	0.0005794
1A''	0.2525762536	6.8729	158.4940	55434.08	180.39	0.0002584
1A'	0.2599927963	7.0748	163.1480	57061.82	175.25	0.0020072
1A'	0.2745919171	7.4720	172.3091	60265.96	165.93	0.0009441
1A'	0.2812158297	7.6523	176.4656	61719.74	162.02	0.0265361
1A''	0.2952624861	8.0345	185.2800	64802.63	154.31	0.0000002
1A'	0.2985657998	8.1244	187.3529	65527.62	152.61	0.0043200
1A'	0.3070324324	8.3548	192.6658	67385.83	148.40	0.0507595

ACCD:

TDDFT EXCITATION ENERGIES

STATE	HARTREE	EV	KCAL/MOL	CM^{-1}	NANOMETERS	OSC. STR.
1A''	0.1202970506	3.2734	75.4875	26402.15	378.76	0.0009760
1A'	0.2071716923	5.6374	130.0022	45468.93	219.93	0.0603261
1A''	0.2237908645	6.0897	140.4309	49116.42	203.60	0.0004698
1A'	0.2345602106	6.3827	147.1888	51480.02	194.25	0.0132936
1A''	0.2477892091	6.7427	155.4901	54383.45	183.88	0.0003126
1A'	0.2540411102	6.9128	159.4132	55755.58	179.35	0.0004667
1A''	0.2570532824	6.9948	161.3034	56416.67	177.25	0.0033601
1A'	0.2583770228	7.0308	162.1341	56707.20	176.34	0.0200827
1A'	0.2622400907	7.1359	164.5582	57555.05	173.75	0.0172405
1A'	0.2692640857	7.3270	168.9658	59096.64	169.21	0.0024398

ACCT:

TDDFT EXCITATION ENERGIES

STATE	HARTREE	EV	KCAL/MOL	CM^{-1}	NANOMETERS	OSC. STR.
1A''	0.1214451144	3.3047	76.2080	26654.12	375.18	0.0010190
1A'	0.2089209799	5.6850	131.0999	45852.86	218.09	0.0595796
1A''	0.2264728332	6.1626	142.1139	49705.04	201.19	0.0004368
1A'	0.2340626276	6.3692	146.8765	51370.81	194.66	0.0122133
1A''	0.2504495808	6.8151	157.1595	54967.33	181.93	0.0002974
1A'	0.2540270199	6.9124	159.4044	55752.49	179.36	0.0061602
1A''	0.2550380990	6.9399	160.0388	55974.39	178.65	0.0031178
1A'	0.2585958703	7.0368	162.2714	56755.23	176.20	0.0076048
1A'	0.2607890669	7.0964	163.6476	57236.58	174.71	0.0206837
1A'	0.2727326837	7.4214	171.1424	59857.91	167.06	0.0023340
1A''	0.2757413510	7.5033	173.0303	60518.23	165.24	0.0240716
1A'	0.2766567721	7.5282	173.6048	60719.14	164.69	0.0028692

This copy of the ESI was uploaded on 13th October 2022, replacing any previous versions published on 20th March 2012

Excitation energies: *Syn* conformer:

Table 6 Calculated excitation energies for the syn-conformer of *t*-BuONO.

CCD:

TDDFT EXCITATION ENERGIES

STATE	HARTREE	EV	KCAL/MOL	CM^{-1}	NANOMETERS	OSC. STR.
1A''	0.1254362479	3.4133	78.7124	27530.07	363.24	0.0011053
1A''	0.2187496950	5.9525	137.2675	48010.01	208.29	0.0000001
1A'	0.2224045480	6.0519	139.5610	48812.16	204.87	0.0373467
1A''	0.2526401817	6.8747	158.5341	55448.11	180.35	0.0001338
1A'	0.2630575148	7.1582	165.0711	57734.45	173.21	0.0055909
1A'	0.2764096805	7.5215	173.4497	60664.91	164.84	0.0024327
1A'	0.2840089431	7.7283	178.2183	62332.76	160.43	0.0162901
1A''	0.2952084126	8.0330	185.2461	64790.76	154.34	0.0015844
1A'	0.2998417149	8.1591	188.1535	65807.65	151.96	0.0826012
1A'	0.3030466808	8.2463	190.1647	66511.06	150.35	0.0631362
1A''	0.3214035408	8.7458	201.6838	70539.92	141.76	0.0036129
1A''	0.3242457901	8.8232	203.4673	71163.73	140.52	0.0005505

ACCD:

TDDFT EXCITATION ENERGIES

STATE	HARTREE	EV	KCAL/MOL	CM^{-1}	NANOMETERS	OSC. STR.
1A''	0.1258413998	3.4243	78.9667	27618.99	362.07	0.0011124
1A''	0.2173180415	5.9135	136.3691	47695.80	209.66	0.0000649
1A'	0.2188506441	5.9552	137.3309	48032.16	208.19	0.0365115
1A'	0.2367794126	6.4431	148.5813	51967.07	192.43	0.0255345
1A''	0.2478190357	6.7435	155.5088	54389.99	183.86	0.0000832
1A'	0.2570456041	6.9946	161.2986	56414.99	177.26	0.0107285
1A''	0.2589736958	7.0470	162.5085	56838.16	175.94	0.0033441
1A'	0.2611529390	7.1063	163.8760	57316.45	174.47	0.0180453
1A'	0.2627603957	7.1501	164.8847	57669.24	173.40	0.0335644
1A'	0.2714005600	7.3852	170.3064	59565.54	167.88	0.0125225
1A'	0.2817150514	7.6659	176.7789	61829.31	161.74	0.0105871
1A''	0.2830643513	7.7026	177.6256	62125.44	160.96	0.0013997

ACCT:

TDDFT EXCITATION ENERGIES

STATE	HARTREE	EV	KCAL/MOL	CM^{-1}	NANOMETERS	OSC. STR.
1A''	0.1272083287	3.4615	79.8244	27919.00	358.18	0.0011747
1A''	0.2193036061	5.9676	137.6151	48131.58	207.76	0.0000626
1A'	0.2207668743	6.0074	138.5333	48452.73	206.39	0.0366882
1A'	0.2364553531	6.4343	148.3780	51895.95	192.69	0.0243054
1A''	0.2508888430	6.8270	157.4351	55063.74	181.61	0.0000620
1A'	0.2571586931	6.9976	161.3695	56439.81	177.18	0.0200829
1A''	0.2571846957	6.9984	161.3859	56445.52	177.16	0.0031305
1A'	0.2603190300	7.0836	163.3527	57133.42	175.03	0.0171069
1A'	0.2627502756	7.1498	164.8783	57667.02	173.41	0.0215348
1A'	0.2749811683	7.4826	172.5533	60351.39	165.70	0.0085704
1A'	0.2791060149	7.5949	175.1417	61256.69	163.25	0.0076549
1A''	0.2806539044	7.6370	176.1130	61596.41	162.35	0.0017355

This copy of the ESI was uploaded on 13th October 2022, replacing any previous versions published on 20th March 2012

Excitation energy of the *t*-BuO radical

Table 7 Calculated exciatation energies and Jahn-Teller splittings (JT-Split) for *t*-BuO.

CAS53	CCD	ACCD	ACCT
Hartree:			
1A'	-231.550708	-231.563879	-231.620467
1A''	-231.550592	-231.563771	-231.620353
2A'	-231.427301	-231.444000	-231.500957
cm^{-1}:			
JT-Split	25.5	23.7	25.0
DE (1A'-2A')	**27084.7**	**26310.4**	**26229.4**

CAS53-PT2			
Hartree:			
1A'	-232.286846	-232.339021	-232.549240
1A''	-232.286890	-232.338481	-232.548647
2A'	-232.158755	-232.220473	-232.430631
cm^{-1}:			
JT-Split	-9.7	118.5	130.1
DE (1A'-2A')	**28112.7**	**26018.3**	**26031.7**

5. NO product branching ratios

Table 8 NO branching ratio for the *t*-BuONO photolysis via its S_2 state for different vibrational states of NO using various REMPI transition states. Due to the nature of the one color experiment, the integral intensity of the vibrational states cannot be compared.

spin-orbit	NO(v'', v')			
state	3,2	1,1	1,0	0,0
$^2\Pi_{1/2}$	0.007	0.279	0.068	0.214
$^2\Pi_{3/2}$	0.003	0.265	0.018	0.146

6. Ion-Maps

This copy of the ESI was uploaded on 13th October 2022, replacing any previous versions published on 20th March 2012

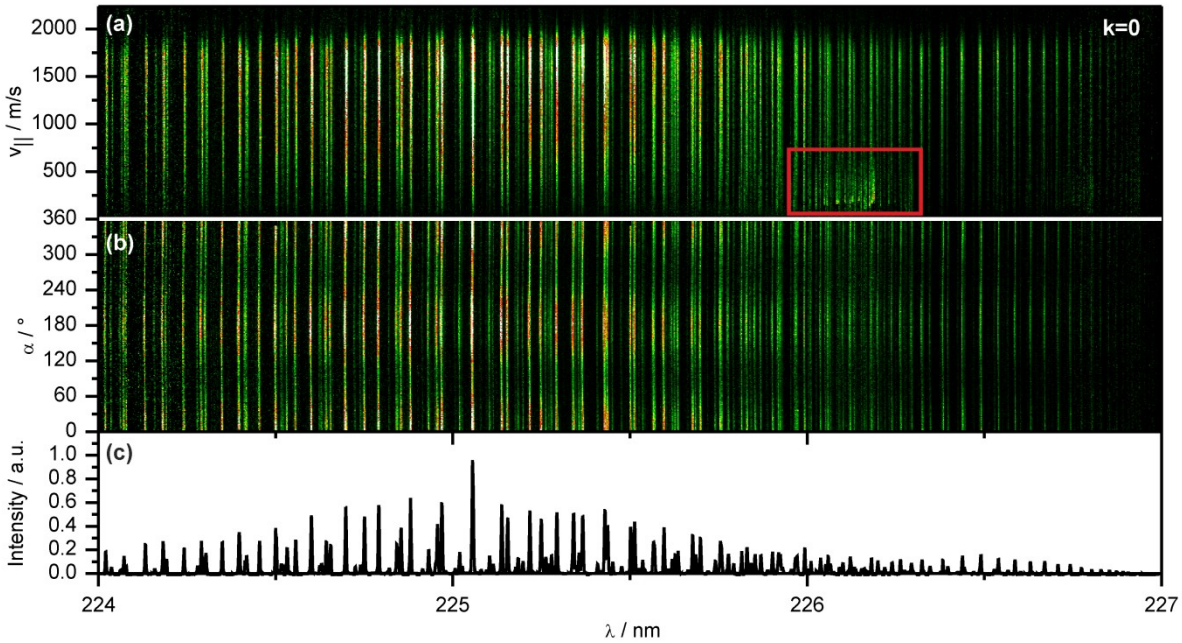

Figure 6 REMPI spectra from the photolysis via the S_1(k = 0) state (λ_{phot} = 398 nm). (a) The 3D-REMPI r-λ-map and (b) the corresponding α-λ -map. (c) Conventional REMPI spectrum obtained by velocity integration of its 3D relative. The red rectangle indicates a region of poor background correction.

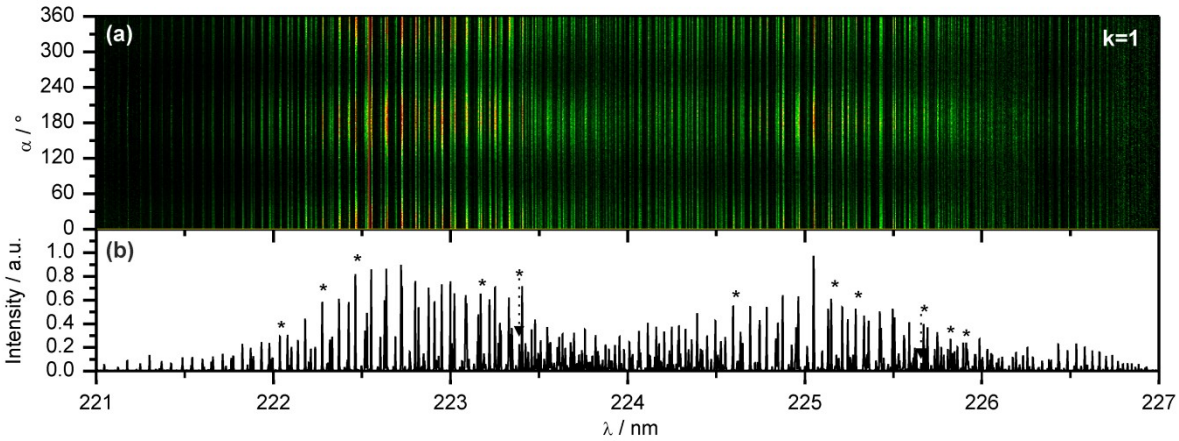

Figure 7 REMPI spectra from the photolysis via the S_1(k = 1) state (λ_{phot} = 381 nm). (a) α-λ -map. (b) Conventional REMPI spectrum obtained by velocity integration of its 3D relative.

This copy of the ESI was uploaded on 13th October 2022, replacing any previous versions published on 20th March 2012

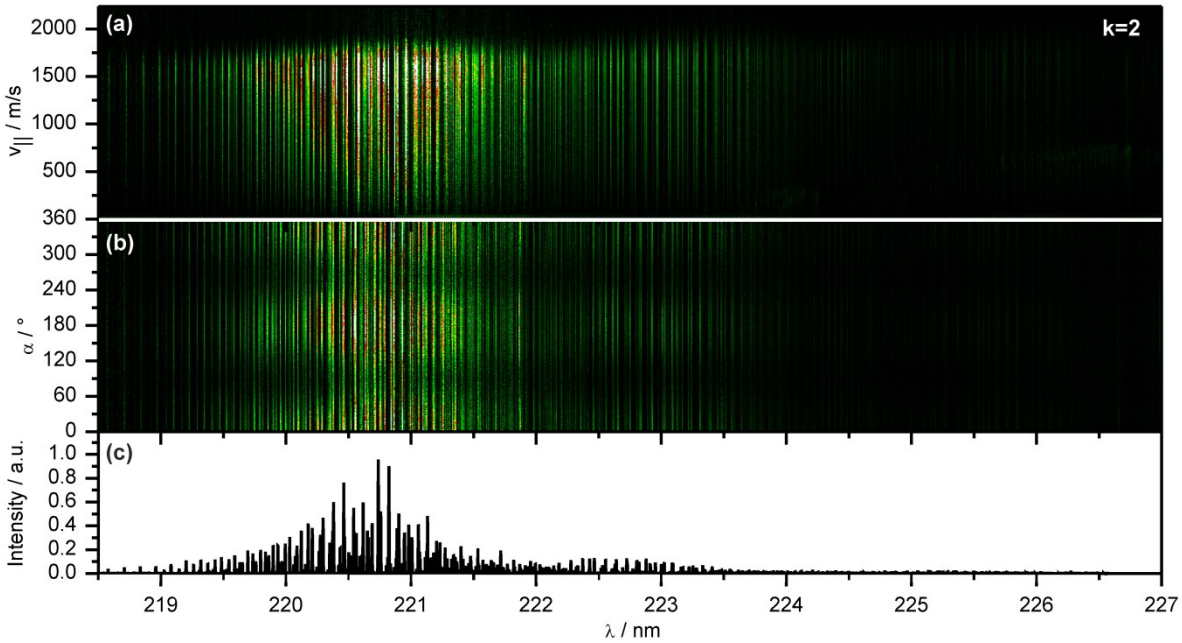

Figure 8 REMPI spectra from the photolysis via the S_1(k = 2) state (λ_{phot} = 365.7 nm). (a) The 3D-REMPI r- λ -map and (b) the corresponding α-λ -map. (c) Conventional REMPI spectrum obtained by velocity integration of its 3D relative.

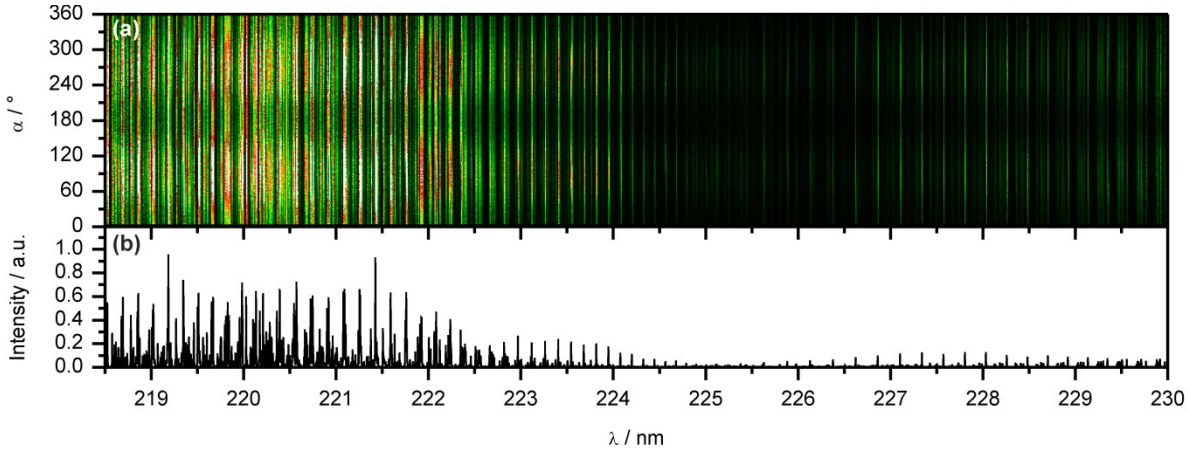

Figure 9 REMPI spectra from the photolysis via the S_2 state (λ_{phot} around 225 nm). (a) α-λ -map. (b) Conventional REMPI spectrum obtained by velocity integration of its 3D relative.

References

1. *Solid Edge V12*, EDS, 2002.
2. E. Wrede, S. Laubach, S. Schulenburg, A. Brown, E. R. Wouters, A. J. Orr-Ewing and M. N. R. Ashfold, *J. Chem Phys.*, 2001, **114**, 2629-2646.
3. A. M. Wenge, U. Kensy and B. Dick, *Phys. Chem. Chem. Phys.*, 2010, **12**, 4644-4655.
4. R. N. Bracewell, *The Fourier Transform and its Applications*, McGraw-Hill New York, 1978.

This copy of the ESI was uploaded on 13th October 2022, replacing any previous versions published on 20th March 2012

5. L. M. Smith, D. R. Keefer and S. I. Sudharsanan, *J. Quant. Spectrosc. Radiat. Transfer*, 1988, **39**, 367-373.
6. C. J. Dasch, *App. Opt.*, 1992, **31**, 1146-1152.
7. G. Pretzler, H. Jäger, T. Neger, H. Philipp and J. Woisetschläger, *Z. Naturforsch.*, 1992, **47a**, 955-970.
8. C. Bordas, F. Paulig, H. Helm and D. L. Huestis, *Rev. Sci. Instrum.*, 1996, **67**, 2257-2268.
9. J. Winterhalter, D. Maier, J. Honerkamp, V. Schyja and H. Helm, *J. Chem. Phys.*, 1999, **110**, 11187-11196.
10. M. J. J. Vrakking, *Rev. Sci. Instrum.*, 2001, **72**, 4084-4089.
11. V. Dribinski, A. Ossadtchi, V. A. Mandelshtam and H. Reisler, *Rev. Sci. Instrum.*, 2002, **73**, 2634-2642.
12. S. Manzhos and H.-P. Loock, *Comp. Phys. Commun.*, 2003, **154**, 76-87.
13. G. A. Garcia, L. Nahon and I. Powis, *Rev. Sci. Instrum.*, 2004, **75**, 4989-4996.
14. G. Herzberg, *Spectra of Diatomic Molecules*, Van Nostrand Reinhold Company New York, 1950.
15. R. N. Zare, *Angular Momentum. Understanding Spatial Aspects in Chemistry and Physics*, John Wiley and Sons Inc., 1988.